J Nanostruct 12(1): 113-122, Winter 2022

RESEARCH PAPER

Influence of Silver and Copper Substitution on Structural, Dielectric, Magnetic, and Catalytic Properties of Nano-Lanthanum Ferrites

Lalitha Ammadu Kolahalam [1], Bhagavatula S Diwakar [2], I.V. Kasi Viswanath [3]*, Venu Reddy [4], N. Krishna Jyothi [5], and Jaya Singh [6]*

[1] *Department of Chemistry, Koneru Lakshmaiah Education Foundation (KLEF), Vaddeswaram, Andhra Pradesh, India*

[2] *Department of Engineering Chemistry, SRKR Engineering College, Andhra Pradesh, India*

[3] *Department of Science & Humanities (Chemistry), NRI Institute of technology, Agiripalli, India*

[4] *Nanotechnology Research Center, SRKR Engineering College, Andhra Pradesh, India*

[5] *Department of Physics, Sri Sathya Sai University for Human Excellence, Kalaburagi, Karnataka, India*

[6] *Department of Chemistry, Banaras Hindu University, Varanasi, Andhra Pradesh, India*

ARTICLE INFO

Article History:
Received 19 July 2021
Accepted 29 November 2021
Published 01 January 2022

Keywords:
Catalytic reduction
Dielectric parameter
Hysteresis loop
Lanthanum ferrite
Saturation magnetization
Silver and copper doping

ABSTRACT

The research paper describes the synthesis of silver, copper doped ($LaXFeO_3$) nano lanthanum ferrites (where X = Ag, Cu, both Ag and Cu) by using the sol-gel method. Their dielectric properties, magnetic properties, and catalytic applications were studied by LCR tester and VSM (Vibrating Sample Magnetometer), UV-Vis Spectroscopy respectively. The dielectric properties were studied as a function of frequency and applied field at room temperature and also in a temperature range of 313 K to 673 K. These results confirmed that the doping of silver and copper decreases the dielectric properties due to their conducting behavior. Room temperature magnetic properties revealed the doping of copper influenced the magnetic properties. It was noticed that the magnetism of bare $LaFeO_3$ is very low and the magnetism of $La_{0.5}Ag_{0.25}Cu_{0.25}FeO_3$ and $La_{0.5}Cu_{0.5}FeO_3$ has increased almost 100 times. This may be attributed to the size and shape of the nano ferrites. Also, the catalytic performance of the doped $LaFeO_3$ nanomaterials showed better catalytic performance. The results indicated that the developed nanostructures will find applications in telecommunications.

How to cite this article
Ammadu Kolahalam L, Diwakar B S, Kasi Viswanath I.V , Reddy V, Krishna Jyothi N, Singh J. Influence of Silver and Copper Substitution on Structural, Dielectric, Magnetic, and Catalytic Properties of Nano-Lanthanum Ferrites. J Nanostruct, 2022; 12(1):113-122. DOI: 10.22052/JNS.2022.01.011

INTRODUCTION

Perovskite oxides ABO_3, composed of rare earth metal A ion with a radius larger than 1.0 Å and transition metal B ion with radius in the order of 0.6 – 0.8 Å, is attained great interest in the modern chemical industry due to its unique properties like high conductivity as well as excellent thermal and chemical stability [1, 2]. Among various ABO_3 type perovskite oxides, the orthorhombic distorted perovskite structured lanthanum ferrite with formula $LaFeO_3$ has gained immense interest under its wide applications in the areas of catalysis

* *Corresponding Author Email: diwakar.b@srkrec.edu.in viswanath.ivk@gmail.com*

as well as electronic and magnetic materials [3, 4].

In recent years, the substitution of metal ions into A- or B-sites of $LaFeO_3$ has been adopted by researchers to provide exciting prospects in improving the dielectric, magnetic and catalytic properties of $LaFeO_3$ [1], [5 – 7]. For instance, Kundu et al. demonstrated that the enhancement of multiferroic and magnetoelectric coupling in $LaFeO_3$ nano-ferrites of samarium substitution [8]. The authors reported a significant change in the magnetic properties in samarium and holmium doped $LaFeO_3$ as compared to the pure $LaFeO_3$ nano-ferrites [8, 9]. In particular, several attempts have been reported in the literature to enhance the catalytic performance of $LaFeO_3$ by substituting the other metals in place of La or Fe of $LaFeO_3$ (1), (5), [10, 11]. The strontium substituted $LaFeO_3$ has shown a significant increase in the catalytic reactions towards the reduction of NO by hydrogen gas [12], methane combustion [13], and N_2O decomposition [14]. The calcium substituted $LaFeO_3$ is also showed excellent catalytic performance for the combustion of methane [15]. Although, many reactions are catalyzed by substituted $LaFeO_3$ nano-ferrites; still, there is a high demand to explore the vast catalytic applicability of substituted $LaFeO_3$ nano-ferrites. This can be achieved by the utilization of substituted $LaFeO_3$ nano-ferrites as a catalyst for other reactions.

The present work was designed to understand the influence of silver and copper doping in the $LaFeO_3$ nano-ferrite. The synthesis was achieved by the sol-gel technique and the structural confirmation can be done by different techniques. To understand the influence of silver and copper on electric and magnetic, catalytic properties were discussed in detail. However, the results are preliminary and a detailed investigation has to be done to understand the mechanism.

MATERIALS AND METHODS

Materials and instruments

Ferric nitrate ($Fe(NO_3)_3.9H_2O$), silver nitrate ($AgNO_3$), cupric nitrate ($Cu(NO_3)_2.3H_2O$), lanthanum nitrate ($La(NO_3)_3.6H_2O$), citric acid ($C_6H_8O_7$), ammonia solution (25% LR) were procured from Merck (India).

The obtained powder samples were characterized by Brukers X-Ray diffraction (XRD) (Brukers AXS D8, USA), Fourier transform infrared (FT-IR) spectroscopy (PerkinElmer/ Spectrum 65), Fourier electron scanning emission microscope (FE-SEM) (NOVA-230, JEOL JSM-7600F FEG-SEM), LCR meter (HIOKI 3532-50, Japan) (vibrating sample magnetometer (VSM) (Lake-shore 7407, USA) and UV-visible Spectroscopy (Lab Man LMSP-UV 1200, India). The energy dispersive X-ray (EDX) data were measured on the FE-SEM coupled with the EDX detector.

Method

In the present work, the $LaFeO_3$ and silver, copper doped $LaFeO_3$ nano-ferrites were prepared by sol-gel technique employing citric acid as stabilizing agent.

Preparation of $LaFeO_3$

To prepare the lanthanum ferrite ($LaFeO_3$) nano-ferrite, the stoichiometric amounts of 4.33 gm of $La(NO_3)_3.6H_2O$, 4.03 gm of $Fe(NO_3)_3.9H_2O$ were dissolved in 100 ml distilled water. The 1.92 gm of citric acid was dissolved in 100 ml of doubled distilled water. In this reaction, citric acid is used as a capping agent to reduce the agglomeration of the particles. These solutions were mixed and stirred vigorously under 80 to 90 ^{0}C followed by the addition of ammonia to maintain the pH 7. The resultant mixture was then heated up to 150 ^{0}C with constant stirring until the formation of a viscous gel. The heating was continued till the formation of a brown colour ash powder. The powder was then calcinated in the air around 900 ^{0}C for 6 hours, subsequently cooled and ground to get a fine powder. The calcinated powder sample was used for characterization.

Preparation of doped $LaFeO_3$ nano-ferrites:

To prepare the silver doped $LaFeO_3$ ($La_{0.5}Ag_{0.5}FeO_3$) nano-ferrite, the stoichiometric amounts of 2.16 gm of $La(NO_3)_3.6H_2O$, 4.03 gm of $Fe(NO_3)_3.9H_2O$, 0.84 gm of $AgNO_3$ were dissolved in 100 ml of double-distilled water. The 1.92 gm of citric acid was dissolved in 100 ml of double-distilled water. Now, the molar ratio of metal nitrates and citric acid solutions was controlled at the ratio of 1:1. Then, these solutions were mixed and stirred vigorously under 80 to 90^{0}C followed by the addition of ammonia solution to maintain the pH 7. The resultant mixture is heated up to 150^{0}C with constant stirring until the formation of a viscous gel. The heating is continued up to the consumption of the whole citrate complex to turn into brown color ash powder.

The prepared powder was calcinated in the air around 900^{0}C for 6 hours, subsequently cooled and ground into fine powder. The sample copper doped $LaFeO_3$ ($La_{0.5}Cu_{0.5}FeO_3$) nano-ferrite was prepared by adding the stoichiometric amount of 1.2gm ($Cu(NO_3)_2.3H_2O$) in place of $AgNO_3$. The other sample silver and copper doped $LaFeO_3$ ($La_{0.5}Ag_{0.25}Cu_{0.25}FeO_3$) nano-ferrite was prepared by varying stoichiometric amount of $AgNO_3$ into 0.42 gm instead of 0.84 gm (in case of $La_{0.5}Ag_{0.5}FeO_3$) and adding a stoichiometric amount of 0.6gm ($Cu(NO_3)_2.3H_2O$).

Catalysis of p-Nitroaniline reduction

0.6906 gm of p-nitroaniline and 0.189 gm of $NaBH_4$ were dissolved in 50 ml of deionized water. Then from this 400 µl of each $NaBH_4$ and p-nitroaniline solutions were dissolved in 3200 µl of deionized water. Take 1500 µl of this reaction mixture into the cuvette which was dissolved in the 1500 µl of deionized water. To this add 0.05 gm of the prepared $LaFeO_3$ and also the doped $LaFeO_3$ powders as the catalysts to the reaction. Now observe the change in the reaction after 10 min employing UV-Visible Spectroscopy.

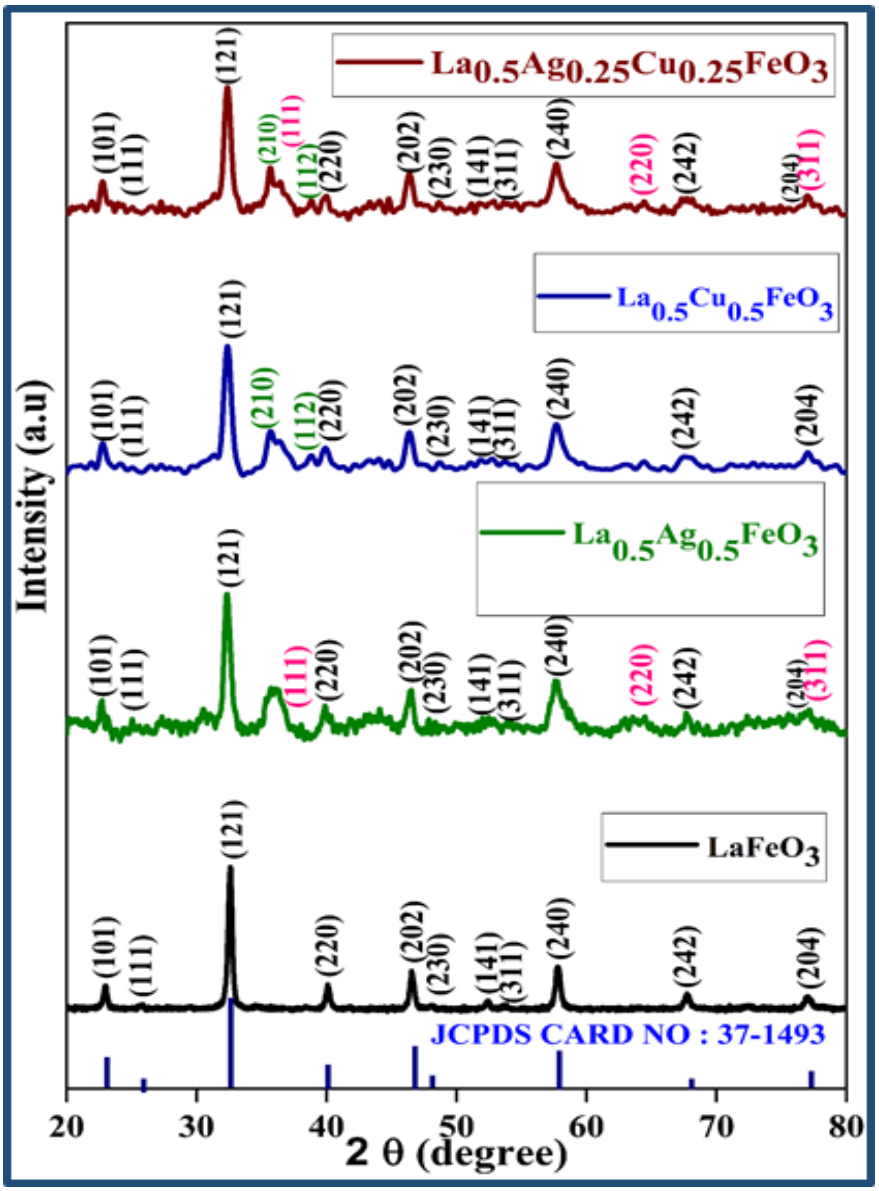

Fig. 1. The XRD patterns of $LaFeO_3$, $La_{0.5}Ag_{0.5}FeO_3$, $La_{0.5}Cu_{0.5}FeO_3$ and $La_{0.5}Ag_{0.25}Cu_{0.25}FeO_3$nano ferrites.

RESULTS AND DISCUSSION

The XRD pattern of the synthesized ferrites was presented in Fig. 1. The XRD patterns of $LaFeO_3$, $La_{0.5}Ag_{0.5}FeO_3$, $La_{0.5}Cu_{0.5}FeO_3$, and $La_{0.5}Ag_{0.25}Cu_{0.25}FeO_3$ revealed that the formation of a single-phase distorted rhombohedral structure in the samples. The patterns of all the four nano ferrites diffraction peaks were matched with the $LaFeO_3$ of JCPDS Card No: 37-1493. Additionally, the $La_{0.5}Ag_{0.5}FeO_3$ nano ferrite showed other peaks related to Ag with miller indices of (111), (220), and (311) planes and matched with the JCPDS Card No: 04-0783 too [16]. $La_{0.5}Cu_{0.5}FeO_3$ nano ferrite showed additional peaks of (210), (112). $La_{0.5}Ag_{0.25}Cu_{0.25}FeO_3$ nano ferrite showed additional peaks of both $La_{0.5}Ag_{0.5}FeO_3$, $La_{0.5}Cu_{0.5}FeO_3$ and this confirmed the presence of doped metals of both Ag and Cu in $La_{0.5}Ag_{0.25}Cu_{0.25}FeO_3$ nano ferrite. These doped ferrite samples had the same symmetry as $LaFeO_3$ with the Pdnm space group. It can be observed from the figure that some peaks of doped ferrite samples become slightly shifted the two theta values in comparison to the $LaFeO_3$ sample. This may be due to the slight variation in the atomic radius of La^{3+}, Ag^{2+}, and Cu^{2+} ions. The size of the synthesized nano ferrites was calculated from the Debye Scherrer equation and all the nano ferrites were in the range of 13 to 22 nm. Individually the size of $LaFeO_3$ nano ferrites was 22 nm, $La_{0.5}Ag_{0.5}FeO_3$ was 15 nm, $La_{0.5}Cu_{0.5}FeO_3$ was 13.2 nm and $La_{0.5}Ag_{0.25}Cu_{0.25}FeO_3$ was 13.6 nm.

The surface morphology of the synthesized nano ferrites was carried out by SEM analysis and presented in Fig. 2. From the figure, the

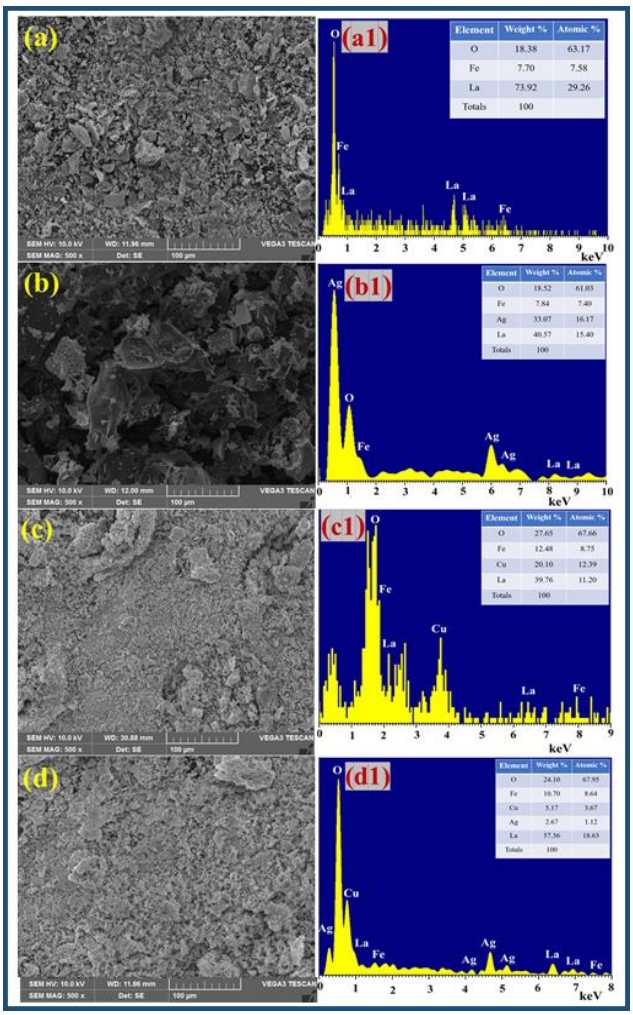

Fig. 2. FE-SEM/EDX spectra of (a/a1) $LaFeO_3$, (b/b1) $La_{0.5}Ag_{0.5}FeO_3$, (c/c1) $La_{0.5}Cu_{0.5}FeO_3$ and (d/d1) $La_{0.5}Ag_{0.25}Cu_{0.25}FeO_3$ nano ferrites.

synthesized $LaFeO_3$ and the doped $LaFeO_3$ nano ferrites of $La_{0.5}Ag_{0.5}FeO_3$, $La_{0.5}Cu_{0.5}FeO_3$, and $La_{0.5}Ag_{0.25}Cu_{0.25}FeO_3$ were little agglomerated and showed a flake-like structure which may be due to the orthorhombic crystal structure. Furthermore, the EDX spectra of all the $LaFeO_3$ nano ferrites were shown in Fig. 2 (a1) – (d1). From the EDX spectrum, each sample of the synthesized $LaFeO_3$ nano ferrites stoichiometric ratio of the constituent chemical composition (La, Ag, Cu, Fe, O) was confirmed and its elemental composition was presented. It was observed that in all the samples La rich environment was observed.These results are in good agreement with the XRD results.

Fig. 3 represents the FTIR spectra of all the four $LaFeO_3$ nano ferrites and its wavenumber ranges from 500 - 4000 cm^{-1}. FT-IR spectroscopy was used for the control of the reaction process and material properties. Therefore, FTIR spectroscopy was performed to know the chemical bonding nature of the constituent elements present in the nano ferrites. The FTIR spectra of $LaFeO_3$ showed two bands correspond to the perovskite phase. In that, the vibrational band around 570 cm^{-1} corresponds to Fe-O stretching vibration (υ_1 mode) and another sharp band around 420 cm^{-1} corresponds to O-Fe-O bending vibrational mode (υ_2 mode). By doping the metals Ag, Cu separately and both Ag, Cu into the $LaFeO_3$ these bands were slightly shifted to the higher wavenumber side [17]. The peaks at 1630 cm^{-1} was attributed to H-O stretching. The existence of sharp peaks in the spectrum indicates the formation of single-phase crystalline compounds. However, the FTIR spectrum of nano ferrites was calcined at 900 ^0C has been confirmed with the orthorhombic structure of $LaFeO_3$. These results were in good agreement with the XRD results.

Dielectric properties

Variation of dielectric constant(ε') with temperature and frequency

The dielectric constant (ε') and dielectric loss (ε") plots were studied over the range of 100 Hz to 5000 Hz. The change in dielectric constant and loss were shown in Fig. 4 and Fig. 5. It is noticed that at lower frequencies all the prepared samples showed higher dielectric constants, particularly $LaFeO_3$ showed the highest value than doped composites. On increasing frequency, the dielectric constant

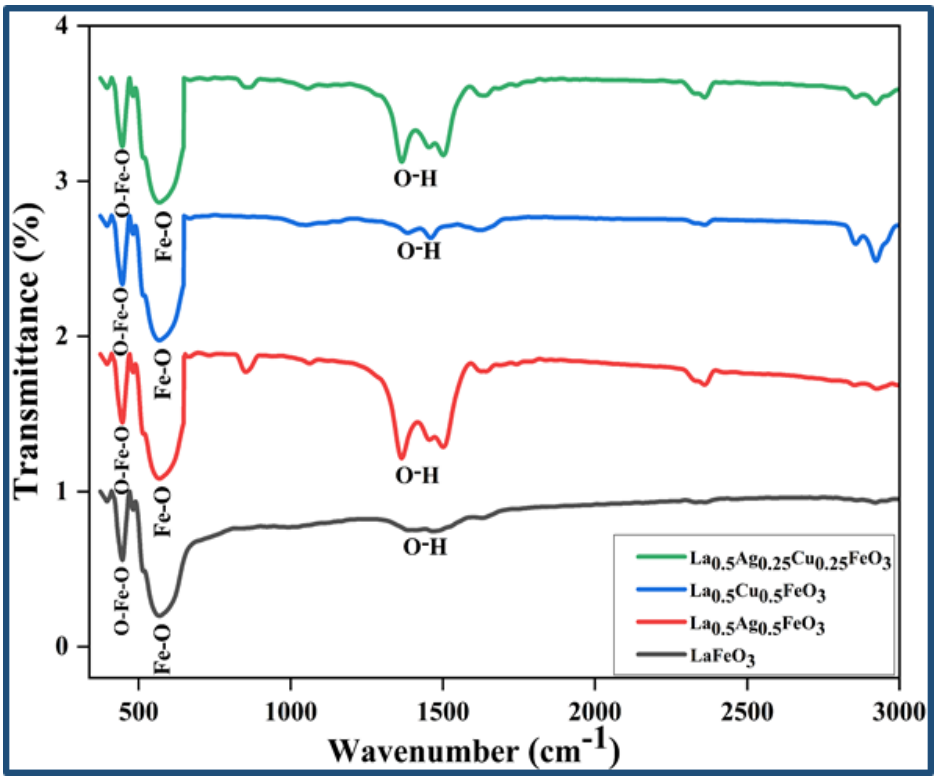

Fig. 3. FT-IR spectra of $LaFeO_3$, $La_{0.5}Ag_{0.5}FeO_3$, $La_{0.5}Cu_{0.5}FeO_3$and $La_{0.5}Ag_{0.25}Cu_{0.25}FeO_3$ nano ferrites.

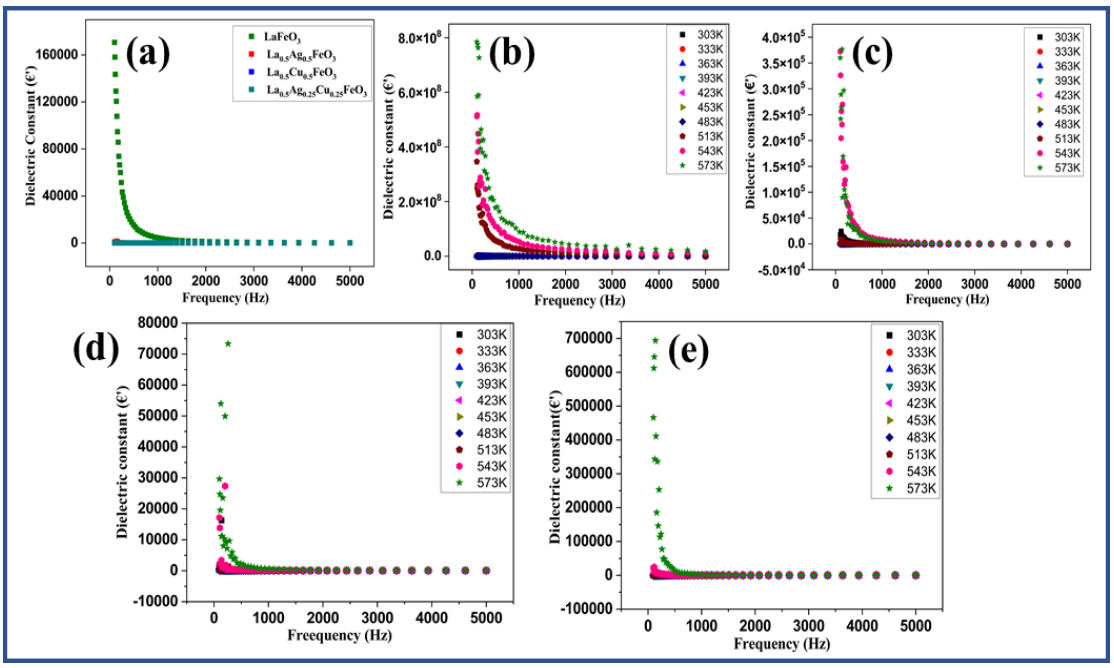

Fig. 4. (a) Variation of Dielectric constant at room temperature for all the four nano ferrites. Variation of dielectric constant with temperature from 303 K to 573 K for (b) $LaFeO_3$, (c) $La_{0.5}Ag_{0.5}FeO_3$ (d) $La_{0.5}Cu_{0.5}FeO_3$ and (e) $La_{0.5}Ag_{0.25}Cu_{0.25}FeO_3$.

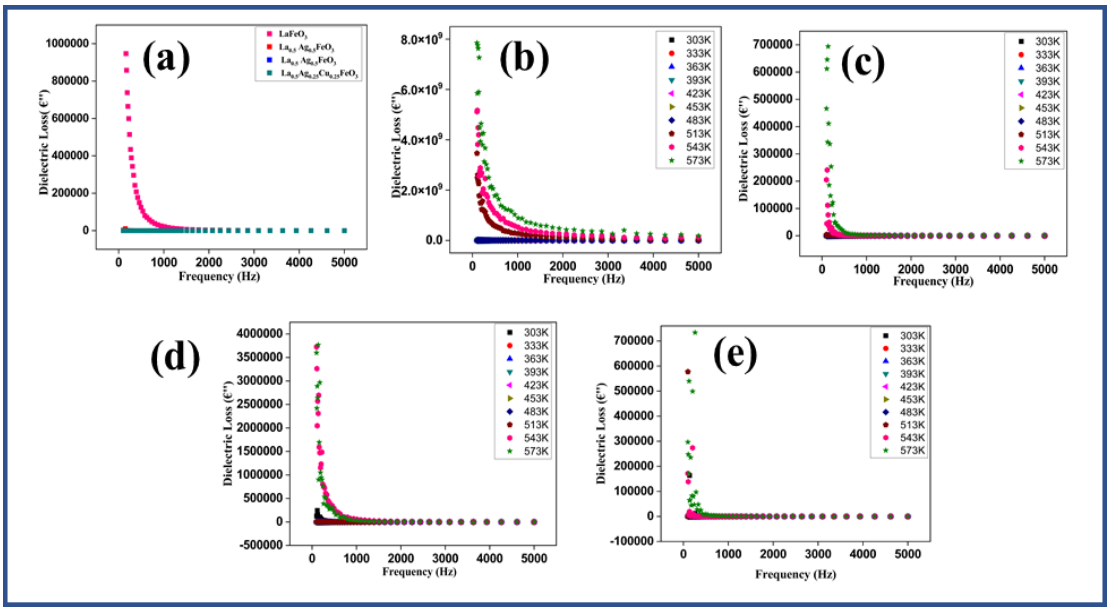

Fig. 5. (a) Variation of dielectric loss at room temperature for all the four nano ferrites. Variation of dielectric loss with temperature from 303 K to 573 K for (b) $LaFeO_3$, (c) $La_{0.5}Ag_{0.5}FeO_3$ (d) $La_{0.5}Cu_{0.5}FeO_3$ and (e) $La_{0.5}Ag_{0.25}Cu_{0.25}FeO_3$.

decreases and attains a constant value. This type of dispersion is called Debye type dispersion, which was a common feature in ferrites. This dispersion was closely related to Maxwell Wagner and two-layer Koop's theory. Due to the effect of space charge polarization the dielectric dispersion occurs. In detail at low frequency, there was the maximum effectiveness of all types of polarizations like interfacial, dipolar, electronic, and ionic which leads to the high dielectric constant value

formation. Whereas on increasing the frequency at a certain point the number of dipoles contributing to the net polarization gets decreased. Because of the assembly of space charge carriers, it requires a certain time to line up their axes parallel to an alternating electric field [18, 19]. This leads to the ineffectiveness of some polarization which shows the direct effect on the net polarization value, then decreased the dielectric constant value. According to Koop's theory [20] at the low-frequency range, the origin of grain boundaries leads to the formation of high resistivity in the sample. Therefore, the value of the dielectric constant increases at this range. In the direction of an applied field, the displacement of an electron occurs on the B site due to the hopping of Fe^{+2} – Fe^{+3}ions. But at a high-frequency range, the low dielectric constant value was observed. Here the dielectric values were reported from the grains of small value with low resistivity which was typical behavior of ferrites [18].

Another reason for the high dielectric constant is due to the presence of oxygen vacancies, defects, and dislocations of the sample [19]. Around 1500 Hz all the samples almost reached a constant value. In the prepared samples the $LaFeO_3$ shows high dielectric constant value than the remaining samples. When the $LaFeO_3$ is doped with silver the value decreased. This may be due to the presence of silver ions which may not be effective for dielectric polarization as the silver has conductance. Surprisingly, the dielectric value of copper doped $LaFeO_3$ is also decreased. This may be due to the influence of the magnetic nature of copper on the surface of $LaFeO_3$. The $LaFeO_3$ is doped with both the metals of silver and copper then the value increased but not more than the $LaFeO_3$. In the doped particles, $La_{0.5}Ag_{0.25}Cu_{0.25}FeO_3$ showed a high dielectric constant value. This implies that in the prepared sample $LaFeO_3$ may work as an efficient device for telecommunication than the doped $LaFeO_3$ [21].

Variation of ε" with temperature and frequency

The dielectric loss (ε") also shows the same trend as dielectric constant. On increasing temperature with frequency, the dielectric loss increases. At low frequencies due to the influence of both charge carriers jump and conduction loss high value of the dielectric loss is observed [22]. On increasing the frequency dielectric loss value decreases up to a certain frequency and then attains almost a constant value.

Magnetic properties

The room temperature magnetic response of the synthesized nano ferrites is depicted in Fig. 6. The evaluation of magnetization in Ag and Cu doped $LaFeO_3$ was achieved with an applied magnetic field of 75 kOe at room temperature.

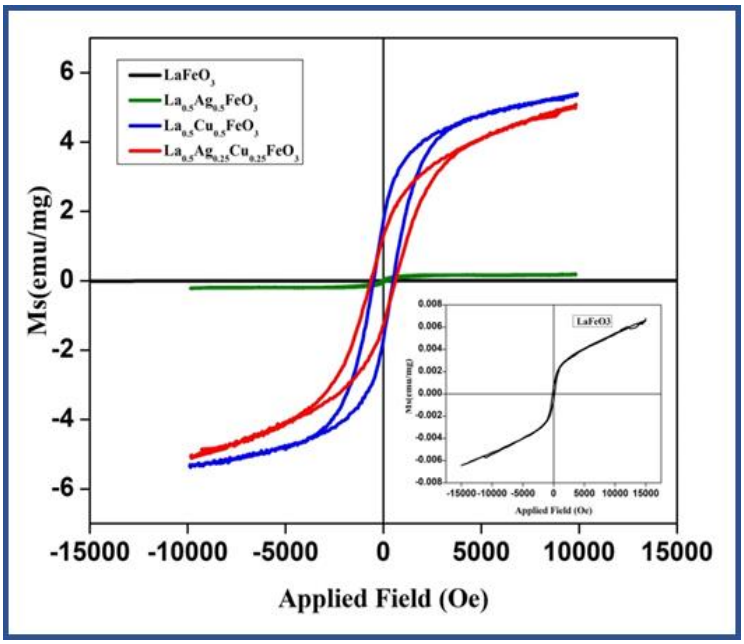

Fig. 6. VSM data of $LaFeO_3$, $La_{0.5}Ag_{0.5}FeO_3$, $La_{0.5}Cu_{0.5}FeO_3$ and $La_{0.5}Ag_{0.25}Cu_{0.25}FeO_3$.

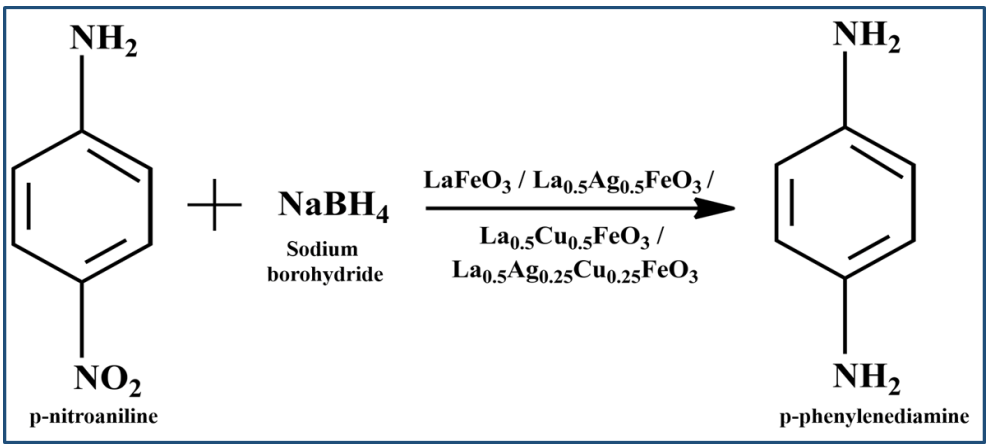

Fig. 7. Reduction of p-nitroaniline into p-phenylenediamine in the presence of $NaBH_4$ and/or with the synthesized nano ferrites.

From the figure it was evident that the hysteresis of $La_{0.5}Cu_{0.5}FeO_3$ nano ferrites showed the highest saturation magnetization, $La_{0.5}Ag_{0.5}FeO_3$ nano ferrites showed the least saturation magnetization among the doped nano ferrites. Whereas the $La_{0.5}Ag_{0.25}Cu_{0.25}FeO_3$ nano ferrites exhibited the saturation magnetization value in between the two individual composites, technically it was nearer to $La_{0.5}Cu_{0.5}FeO_3$. The same phenomenon is observed in the case of remanence but the coercivity of the $La_{0.5}Cu_{0.5}FeO_3$ nanoparticles is high. It was also noticed that the magnetism of bare $LaFeO_3$ is very low and the magnetism of $La_{0.5}Ag_{0.25}Cu_{0.25}FeO_3$ and $La_{0.5}Cu_{0.5}FeO_3$ has increased almost 100 times. This may be attributed to the size and shape of the nano ferrites. According to Brown's relation, the coercivity is inversely proportional to the magnetic saturation which is obeyed by the samples [23]. Also, it is a well-known fact that the change in the coercivity of the nano ferrites can be explained by grain sizes. As the size is small, the magnetic anisotropy of the hard grains is averaged because of exchange coupling. This coupling strengthens the ferromagnetic component and the presence of oxygen vacancies can also disturb the exchange coupling interactions thus increases the ferromagnetism. From the structural characterization, it was noticed that the doping of copper in lanthanum ferrite, the magnetic core from copper is more on the surface of the particles which may cause the uncompensated surface spins which contribute to the increase in magnetization. On the other hand, the M-H curve of $La_{0.5}Ag_{0.5}FeO_3$ composite exhibited an almost paramagnetic nature due to the presence of electrically conductive silver is present in it which causes a decrease in coercivity and an increase in remnant magnetization.

Catalytic properties

The reaction in the Fig. 7 displays the reduction of p-nitroaniline into p-phenylenediamine in the presence of $NaBH_4$ in aqueous solutions and with $LaFeO_3$, $La_{0.5}Ag_{0.5}FeO_3$, $La_{0.5}Cu_{0.5}FeO_3$ and $La_{0.5}Ag_{0.25}Cu_{0.25}FeO_3$ samples.

The formation of p-phenylenediamine in the presence of $LaFeO_3$, $La_{0.5}Ag_{0.5}FeO_3$, $La_{0.5}Cu_{0.5}FeO_3$ and $La_{0.5}Ag_{0.25}Cu_{0.25}FeO_3$ samples were studied by UV-visible spectroscopy (Fig. 8). Initially, a blank reaction was carried out without the developed nano ferrites to understand the influence of $NaBH_4$. It was noticed that even after 60 mins there was no change in the reactant concentration and no new peak observed in the UV Vis spectra. Later the reaction was performed with the addition of synthesized nanoparticles. Since there was no observable change noticed in the reaction up to 10 min, it was taken as the optimum time to study. The UV–visible spectrum of the reaction mixture without nano ferrites (curve i) showed two absorption peaks at 383nm and 226 nm that correspond to p-nitroaniline. While observing Fig. 8 (a) and (b) there was no observable change in the UV–visible spectrum of $LaFeO_3$, $La_{0.5}Ag_{0.5}FeO_3$. But in the case of $La_{0.5}Cu_{0.5}FeO_3$ and $La_{0.5}Ag_{0.25}Cu_{0.25}FeO_3$ samples, there was a notable change in the UV–visible spectrum of the reaction mixture. From Fig. 8 (c) and (d), the reaction mixture containing nano ferrites (curve ii) with a reaction period of 10 minutes showed the decrease in the characteristic

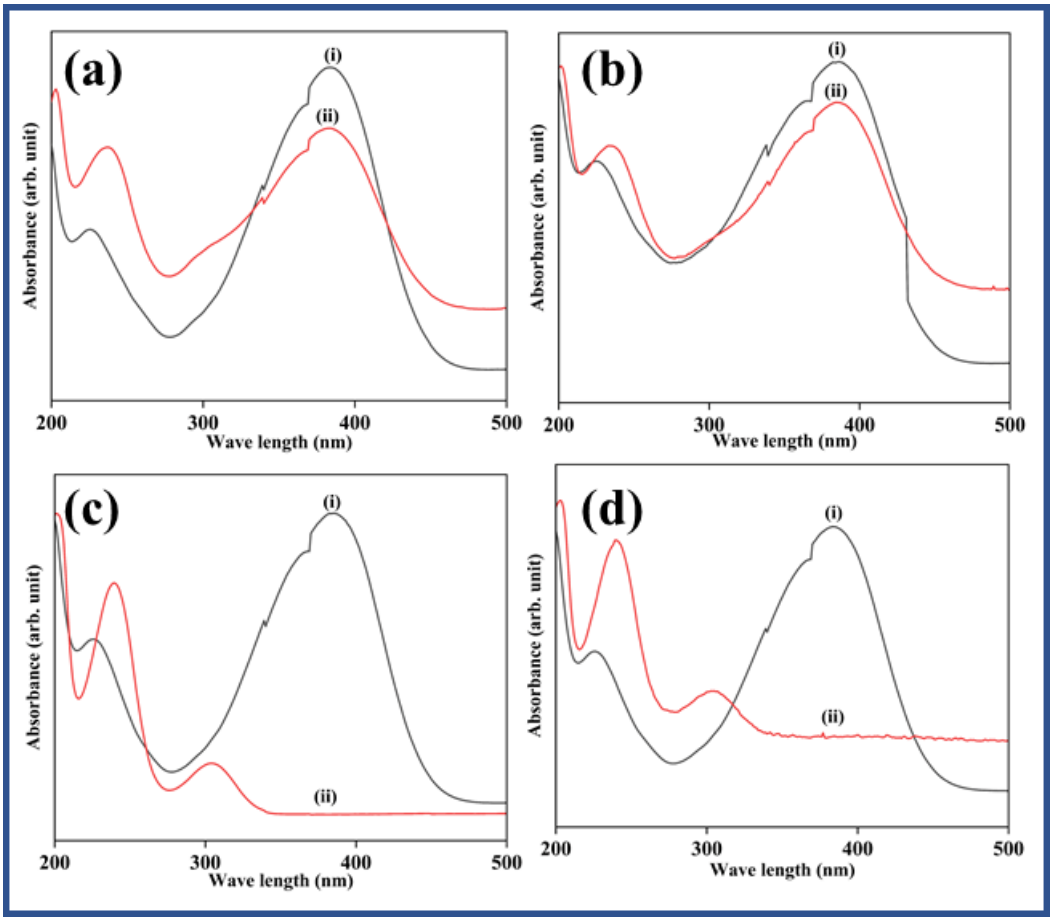

Fig. 7. UV-visible spectra of Catalytic reduction of p-nitroaniline (curve i) without and (curve ii) with (a) $LaFeO_3$, (b $La_{0.5}Ag_{0.5}FeO_3$, (c) $La_{0.5}Cu_{0.5}FeO_3$ and (d) $La_{0.5}Ag_{0.25}Cu_{0.25}FeO_3$ nano ferrites

peak of p-nitro aniline at 383 nm [24] shift in the absorbance peak at 226 nm and appearance of a new peak at 305 nm. This result indicated that the $La_{0.5}Cu_{0.5}FeO_3$and $La_{0.5}Ag_{0.25}Cu_{0.25}FeO_3$ nanomaterials accelerated the reduction reaction of p-nitroaniline with $NaBH_4$ in aqueous solutions by the formation of p-phenylenediamine. The percentage conversion of p-nitroaniline to p-phenylenediamine is 86% in the presence of $La_{0.5}Cu_{0.5}FeO_3$ and 100 % in the presence of $La_{0.5}Ag_{0.25}Cu_{0.25}FeO_3$. This result suggests that as prepared $La_{0.5}Ag_{0.25}Cu_{0.25}FeO_3$ sample showed better catalytic properties than the $La_{0.5}Cu_{0.5}FeO_3$ sample. However further studies are required to understand the kinetics of the reaction.

CONCLUSIONS

Cu and Ag doped nano size lanthanum ferrites were synthesized effectively by using the sol-gel method. The XRD pattern confirmed orthorhombic crystal structure and size of all the synthesized nano ferrites were in the range of 13 to 22 nm. There was a good correlation between the XRD, SEM/EDX and FT-IR data. The prepared nano ferrites showed good results of magnetic, dieelectric properties which can be useful in the application of telecommunication devices, optical materials. Furthermore, these developed nano ferrites were studied their catalytic reduction of p-nitroaniline and among the synthesized nanoferrites $La_{0.5}Ag_{0.25}Cu_{0.25}FeO_3$ exhibited prominent catalytic activity to reduce p-nitroaniline into p-phenylenediamine. However, further studies are required to explore the samples.

ACKNOWLEDGMENTS

One of the authors (Lalitha Ammadu Kolahalam) is thankful to Koneru Lakshmaiah Education Foundation, Vaddeswaram (A.P) India,

for providing necessary laboratory facilities and financial support to carry out this work.

CONFLICT OF INTEREST

The authors declare that there is no conflict of interests regarding the publication of this manuscript.

REFERENCE

1. Parrino F, García-López E, Marcì G, Palmisano L, Felice V, Sora IN, et al. Cu-substituted lanthanum ferrite perovskites: Preparation, characterization and photocatalytic activity in gas-solid regime under simulated solar light irradiation. Journal of Alloys and Compounds. 2016;682:686-694.
2. Roth RS. Classification of perovskite and other ABO_3-type compounds. JRNBS. 1957;58(2):75.
3. Furfori S, Bensaid S, Russo N, Fino D. Towards practical application of lanthanum ferrite catalysts for NO reduction with H_2. Chem Eng J. 2009;154(1-3):348-354.
4. Mihai O, Chen D, Holmen A. Catalytic Consequence of Oxygen of Lanthanum Ferrite Perovskite in Chemical Looping Reforming of Methane. Industrial & Engineering Chemistry Research. 2010;50(5):2613-2621.
5. Jauhar S, Singhal S. Chromium and copper substituted lanthanum nano-ferrites: Their synthesis, characterization and application studies. Journal of Molecular Structure. 2014;1075:534-541.
6. Desai P, Athawale A. Microwave Combustion Synthesis of Silver Doped Lanthanum Ferrite Magnetic Nanoparticles. Def Sci J. 2013;63(3):285-291.
7. Mitra A, Mahapatra AS, Mallick A, Shaw A, Bhakta N, Chakrabarti PK. Improved magneto-electric properties of $LaFeO_3$ in $La_{0.8}Gd_{0.2}Fe_{0.97}Nb_{0.03}O_3$. Ceram Int. 2018;44(4):4442-4449.
8. Kundu SK, Rana DK, Karmakar L, Das D, Basu S. Enhanced multiferroic, magnetodielectric and electrical properties of Sm doped Lanthanum ferrite nanoparticles. Journal of Materials Science: Materials in Electronics. 2019;30(11):10694-10710.
9. Mahapatra AS, Mitra A, Mallick A, Ghosh M, Chakrabarti PK. Enhanced magnetic property and phase transition in Ho^{3+} doped $LaFeO_3$. Materials Letters. 2016;169:160-163.
10. Ansari AA, Ahmad N, Alam M, Adil SF, Assal ME, Albadri A, et al. Optimization of Redox and Catalytic Performance of $LaFeO_3$ Perovskites: Synthesis and Physicochemical Properties. Journal of Electronic Materials. 2019;48(7):4351-4361.
11. Gao Y, Yang G, Dai Y, Li X, Gao J, Li N, et al. Electrodeposited Co-Substituted $LaFeO_3$ for Enhancing the Photoelectrochemical Activity of $BiVO_4$. ACS Applied Materials & Interfaces. 2020;12(15):17364-17375.
12. Tarjomannejad A, Niaei A, Gómez MJI, Farzi A, Salari D, Albaladejo-Fuentes V. NO + CO reaction over LaCu0.7B0.3O3 (B = Mn, Fe, Co) and $La_{0.8}A_{0.2}Cu_{0.7}Mn_{0.3}O_3$ (A = Rb, Sr, Cs, Ba) perovskite-type catalysts. Journal of Thermal Analysis and Calorimetry. 2017;129(2):671-680.
13. Zhang X, Li H, Li Y, Shen W. Structural Properties and Catalytic Activity of Sr-Substituted $LaFeO_3$ Perovskite. Chinese Journal of Catalysis. 2012;33(7-8):1109-1114.
14. Mokhtar M, Medkhali A, Narasimharao K, Basahel S. Divalent Transition Metals Substituted $LaFeO_3$ Perovskite Catalyst for Nitrous Oxide Decomposition. Journal of Membrane and Separation Technology. 2014;3(4):206-212.
15. Ciambelli P, Cimino S, Lisi L, Faticanti M, Minelli G, Pettiti I, et al. La, Ca and Fe oxide perovskites: preparation, characterization and catalytic properties for methane combustion. Applied Catalysis B: Environmental. 2001;33(3):193-203.
16. Wei W, Guo S, Chen C, Sun L, Chen Y, Guo W, et al. High sensitive and fast formaldehyde gas sensor based on Ag-doped $LaFeO_3$ nanofibers. Journal of Alloys and Compounds. 2017;695:1122-1127.
17. Andoulsi-Fezei R, Horchani-Naifer K, Férid M. Influence of zinc incorporation on the structure and conductivity of lanthanum ferrite. Ceram Int. 2016;42(1):1373-1378.
18. Manzoor A, Khan MA, Shahid M, Warsi MF. Investigation of structural, dielectric and magnetic properties of Ho substituted nanostructured lithium ferrites synthesized via auto-citric combustion route. Journal of Alloys and Compounds. 2017;710:547-556.
19. Ishaque M, Islam MU, Azhar Khan M, Rahman IZ, Genson A, Hampshire S. Structural, electrical and dielectric properties of yttrium substituted nickel ferrites. Physica B: Condensed Matter. 2010;405(6):1532-1540.
20. Koops CG. On the Dispersion of Resistivity and Dielectric Constant of Some Semiconductors at Audiofrequencies. Physical Review. 1951;83(1):121-124.
21. Andoulsi-Fezei R, Sdiri N, Horchani-Naifer K, Férid M. Effect of temperature on the electrical properties of lanthanum ferrite. Spectrochimica Acta Part A: Molecular and Biomolecular Spectroscopy. 2018;205:214-220.
22. Saad Y, Hidouri M, Álvarez-Serrano I, López ML, Toulemonde O, Wattiaux A, et al. Dielectric response of ceramic $Sr_{2-x}Bi_xTi_{2-x}Fe_xO_6$ (0≤x≤1.5) perovskites. Journal of Physics and Chemistry of Solids. 2015;81:40-49.
23. Nongjai R, Khan S, Asokan K, Ahmed H, Khan I. Magnetic and electrical properties of In doped cobalt ferrite nanoparticles. Journal of Applied Physics. 2012;112(8):084321.
24. Reddy V, Torati RS, Oh S, Kim C. Biosynthesis of Gold Nanoparticles Assisted by Sapindus mukorossi Gaertn. Fruit Pericarp and Their Catalytic Application for the Reduction of p-Nitroaniline. Industrial & Engineering Chemistry Research. 2012;52(2):556-564.